

X-Ray Microanalysis of Cryopreserved Human Skin to Study the Effect of Iontophoresis on Percutaneous Ion Transport¹

Louk A. R. M. Pechtold,² Harry E. Boddé,^{2,3}
Hans E. Junginger,² Henk K. Koerten,⁴ and
Joke A. Bouwstra^{2,5}

Received February 22, 2001; accepted April 15, 2001

Purpose. To study at the ultrastructural level which part of the skin is associated with percutaneous iodide transport by passive diffusion and iontophoresis.

Methods. Following passive diffusion or iontophoresis of iodide, the morphology and the ion distribution of the skin was preserved by rapid freezing. The skin was kept frozen until and during examination by transmission electron microscopy (TEM) and X-ray microanalysis (XRMA). The intrinsic electron absorbing characteristics of cryopreserved skin allow direct TEM examination without additional staining. XRMA can be used to obtain in a relatively nondestructive way *in situ* information on ion distributions across the skin.

Results. After passive diffusion, iodide was mainly found in the stratum corneum (SC), whereas there was little iodide in the viable epidermis. Iontophoresis up to 300 $\mu\text{A}/\text{cm}^2$ did not significantly affect this distribution. With iontophoresis at 1000 $\mu\text{A}/\text{cm}^2$, the amount of iodide increased dramatically and was equally distributed over the SC and viable epidermis. The presence of iodide in the SC suggests that iodide is present inside corneocytes.

Conclusions. Iontophoresis up to 300 $\mu\text{A}/\text{cm}^2$ does not significantly perturb skin structures in contrast to iontophoresis at 1000 $\mu\text{A}/\text{cm}^2$. The presence of iodide inside corneocytes suggests the possibility of transcellular percutaneous iodide transport.

KEY WORDS: iontophoresis; passive diffusion; stratum corneum; ion transport; X-ray micro analysis; cryopreservation; transmission electron microscopy.

INTRODUCTION

The upper layer of the human skin, the stratum corneum (SC), is generally recognized as the major barrier to the percutaneous diffusion of water and hydrophilic compounds (1,2). Applying an electric potential gradient across the skin, as with iontophoresis, enhances the transport of hydrophilic compounds through the skin (2,3). Despite much research on the applicability of this technique for drug delivery, still little is known about the precise pathways these compounds follow across the SC during passive diffusion and iontophoresis.

Transmission electron microscopy (TEM) is a valuable tool in studying the transport of ions through the skin (4–9). Combined with the use of chemicals to preserve the skin and to visualize the location of the migrating ions by precipitation, insightful information was obtained on which structures were associated with ion transport by passive diffusion and iontophoresis. Indirectly, this information indicated the pathways taken by the migrating ions. However, when studying percutaneous ion transport, the use of chemicals may be questionable, as chemicals have been reported to be able to dislocate ions in biological tissue (10). Furthermore, visualizing the locations of ions by chemical precipitation may entail artifacts, as the observed ion distribution may be a function of precipitation kinetics (9,11).

An alternative to preserving skin and its ion distribution by chemicals is cryopreservation. Rapid freezing instantaneously stabilizes the tissue morphology and immobilizes the ions (12). Successive cryohandling of the frozen sample allows investigation of the morphology and preserves the distribution of ions (12). The intrinsic electron absorbing characteristics of cryopreserved skin allows direct TEM examination without additional staining (13,14). In such material, X-ray microanalysis (XRMA) may serve to study ion localization. Application of XRMA allows *in situ* information on the element distribution in a specimen to be obtained. Hence, it becomes possible to study ion distributions across skin in a relatively nondestructive way (4,13,14).

In the present study we performed XRMA in TEM on cryopreserved skin to establish at the ultrastructural level which part of the skin is associated with percutaneous iodide transport by passive diffusion and iontophoresis. In this study we chose iodide as the transportation because this ion has been used in a previous related study using fluorescence spectroscopy (15).

MATERIALS AND METHODS

Chemicals

HEPES (4-(2-hydroxyethyl)-1-piperazineethanesulfonic acid) and sodium chloride (NaCl) were purchased from Sigma Chemical Co. (St. Louis, MO); silver wire (Ag), 1 mm diameter, 99.9% w/w pure, from Aldrich Chemical Co. (Milwaukee, WI); silver iodide (AgI), 99.9% w/w pure, from Acros (Geel, Belgium); potassium iodide (KI), sodium thiosulfate ($\text{Na}_2\text{S}_2\text{O}_3$), silver nitrate (AgNO_3), and Y-Eosine from Merck (Darmstadt, Germany); 1-octanol from Baker (Deventer, The Netherlands); and agar from Difco Laboratories (Detroit, MI). Bi-distilled water was used.

KI-Agar Gel Standards

To obtain KI-agar gels containing 0.0, 0.056, 0.11, 0.56, and 1.1 M KI, first a 7% (w/w) solution of agar was heated up to 100°C. Then this solution was cooled to 50°C and subsequently mixed with the same volume of a KI solution of a known concentration (containing 0.1% (w/w) $\text{Na}_2\text{S}_2\text{O}_3$) so that the desired concentration KI in gel was obtained. Finally the KI-agar solution was allowed to gel at 4°C.

Partition Experiments

KI was subject to partition studies using 0.55 M KI as the aqueous phase, and 1-octanol, being a model for skin lipids, as

¹ This article is dedicated to the memory of Harry H. Boddé, deceased on September 8, 1996.

² Leiden Amsterdam Center for Drug Research, Division of Pharmaceutical Technology, Leiden, The Netherlands.

³ Deceased.

⁴ Center for Electron Microscopy, Leiden University Medical Center, Leiden, The Netherlands.

⁵ To whom correspondence should be addressed at LACDR, division of Pharmaceutical Technology, PO Box 9502, 2300 RA Leiden, The Netherlands. (e-mail: bouwstra@chem.leidenuniv.nl)

the organic phase. Equilibrium partitioning was achieved by shaking the KI-octanol mixture. To determine how much iodide had partitioned into the 1-octanol, the organic phase was exposed to reverse extraction using water. Actual iodide concentrations were determined by a titration using Y-Eosin and AgNO_3 . The experiment was carried out in quadruple.

Skin Preparation

Freshly excised abdominal skin was obtained from cosmetic surgery. After removal of the subcutaneous fat, the skin was dermatomed to a thickness of approximately 200 μm using a Padgett Dermatome (Kansas City Assemblage Co., Kansas City, MO, USA).

Passive Diffusion Experiments

The skin was mounted in a perspex side-by-side diffusion cell (Gorlaeus Laboratories, Leiden, The Netherlands). This cell consisted of a donor and an acceptor compartment between which a piece of skin could be clamped. The skin surface area facing the donor and acceptor phase was 0.6 cm^2 .

To study iodide localization in the skin due to passive diffusion, the SC side was exposed to a 1.1 M KI solution (containing 0.1% (w/w) $\text{Na}_2\text{S}_2\text{O}_3$, pH 6) for 10 h, while the viable epidermal side was exposed to HEPES buffer (20 mM HEPES, 50 mM NaCl, pH 7.4). Skin of which both sides had been exposed to the HEPES buffer for 10 h served as a control.

Iontophoresis Experiments

Iontophoresis was carried out using the same diffusion cell as used for the diffusion experiments. The donor compartment (facing the SC) contained a 1.1 M KI solution, whereas the acceptor compartment (facing the viable epidermis) contained HEPES buffer. Iontophoresis was carried out with a silver (Ag) anode and a silver/silver iodide (Ag/AgI) cathode. The cathode was prepared by coating a silver wire with molten silver iodide. The electrodes were placed in separated vials, which were electrically connected with the donor and acceptor compartments by high conductivity salt-bridges. The vial in which the cathode was placed contained a 1.1 M KI solution, whereas the vial housing the anode was filled with HEPES buffer. The salt-bridges were medical PVC tubes (2 mm in diameter, 8 cm long) filled with agar gel prepared according to the procedure previously described. The salt-bridge at the donor side was prepared from 3.5% (w/w) agar containing 1.1 M KI, whereas the one at the anodal side was prepared from 3.5% (w/w) agar containing 20 mM HEPES and 1 M NaCl (buffered at pH 7.4).

To study the effects of an electric field on iodide localization in the skin, the skin was subjected to a constant current of 100, 300, or 1000 $\mu\text{A}/\text{cm}^2$ for 10 h. The current was delivered by a programmable current source (CED-Gorlaeus Laboratories, Leiden, The Netherlands) that provided constant adjustment and monitoring of the voltage or current throughout the experiment.

Sample Preparation for TEM

After the experiment was finished, the skin was removed from the diffusion cell and cut into samples of $1 \times 1 \times 0.2$ mm. The samples were cryofixed in liquid propane using the plunging method (KF80; Reichert-Jung, Vienna, Austria). Subsequently, the samples were stored in liquid nitrogen. The

time lapse between termination of the experiment and freezing of the samples was about 10 min. At -160°C , thin sections were sliced from the frozen samples using a Reichert FCS cryo-ultra microtome (Leica, Germany) set at 250 nm. The cryosections were collected on copper grids (300 mesh). The grids were covered by a carbon-coated pioloform membrane and stored at -180°C . Using a cryospecimen transfer holder (Gatan Inc., Pleasanton, CA, USA) the grids were cryotransferred to a Philips EM 400 TEM (Philips, Eindhoven, The Netherlands) and examined at -170°C . The sample preparation of KI-agar gels was similar to that of the skin.

XRMA

Iodide localization in the samples was studied by XRMA using a TN 2000 X-ray microanalyzer (Tracor Northern, Middleton, WI, USA), which was attached to the microscope. Each analysis comprised the collection of X-rays from a focused electron beam (140 nm diameter) during 200 s. For this purpose an accelerating voltage of 100 KeV and a beam current of 0.125 μA were used. To reduce extraneous X-rays, copper grids were placed in a beryllium specimen holder and tilted 18° toward the detector. Freeze-drying of the cryosections was minimized by limiting the total examination time of a copper grid to 1.5 h.

The presence of iodide was established from its $L_{\alpha 1}$ emission by collecting the total X-ray counts between 3.76 and 4.16 KeV. To obtain a semiquantitative estimation of the elemental concentration corrected for variations in section thickness, iodide peak-to-background ratios (P/BG) were calculated. Hereby the peak (P) was defined as the collected iodide X-ray counts that were superimposed on the continuum of background radiation in the X-ray spectrum. A least square fitting method (16) was used to calculate the baseline under the peak. The background (BG) was defined as the collected X-ray counts below the baseline.

Statistical Analysis

To determine significant differences among data points, the data were analyzed using an analysis of variance test followed by Tukey's multiple comparison test (Prisma statistical computer program, GraphPad Software Inc., San Diego, CA). The significance of a linear trend among data points was established using a linear regression analysis. To decide whether two groups of data significantly differed from each other, an unpaired two-tailed Student's *t*-test was used. For all tests significance was determined using a 95% confidence level.

RESULTS

TEM

Figure 1a shows the ultrastructure of cryopreserved skin, which had been exposed to passive diffusion by 1.1 M KI. Similar results were obtained with skin preserved after iontophoresis or HEPES diffusion experiments. Cryosections allowed clear discrimination between the SC and the underlying tissue of the viable epidermis. The SC could be identified by the characteristic stretched, flattened corneocytes with an electron lucent intracellular space. Corneocytes were closely attached to each other by electron dense material, which did not reveal any ultrastructure. Sectioning of the frozen tissue frequently resulted in the loss of corneocyte layers. Only the six to seven most proximal corneocyte layers remained in

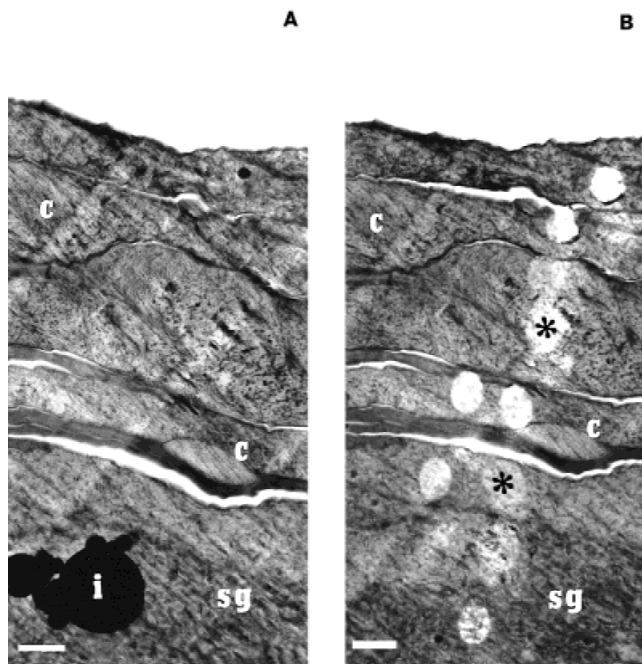


Fig. 1. (A) Transmission electron micrograph of cryopreserved skin after 10 h exposure to KI diffusion. The upper part shows the SC with about six layers of corneocytes (C). The lower part shows the stratum granulosum (SG). The micrograph also shows an ice particle (i). (B) The same part of the skin shown in Fig. 1a after examination by XRMA spot analysis (*). Scale bar represents 2 μm .

direct contact with the viable epidermis. Usually, cells of the viable epidermis showed freezing damage. Sometimes, however, layers of the stratum granulosum were relatively well preserved, showing cells in which nuclei could be distinguished. In general the freezing artifacts were such that, due to the spot size of the electron beam (140 nm in diameter), mean values for P/BG ratios of iodide could still be obtained. Comparison of the structure of the SC and of the viable epidermis showed no difference between skin that was subjected to HEPES diffusion, KI diffusion, or KI iontophoresis.

XRMA of KI-Agar Gel Standards

Cryosections of the KI-agar gel standards were examined by TEM. No crystals could be identified even in gels containing 1.1 M KI. To establish a calibration line, randomly selected spots on the cryosections were measured by XRMA. The spot of analysis on the cryosections became electron lucent from irradiation during XRMA, yet repeated measurements on the same spot showed no significant decrease in iodide X-ray count yield. The statistical evaluation included only those P/BG ratios that were significantly higher than the level of background noise, defined as three times the standard deviation of P/BG ratios obtained from 0.0 M KI gel (17). Figure 2 displays the significant P/BG ratios plotted as a function of the KI concentration per gel. As can be observed, from 0.056 to 1.1 M KI, the P/BG ratio increased linearly with the KI concentration. Thus, a calibration line was formed.

XRMA of Skin

The presence of iodide across the skin was studied by XRMA spot analysis, each spot close to the previous spot.

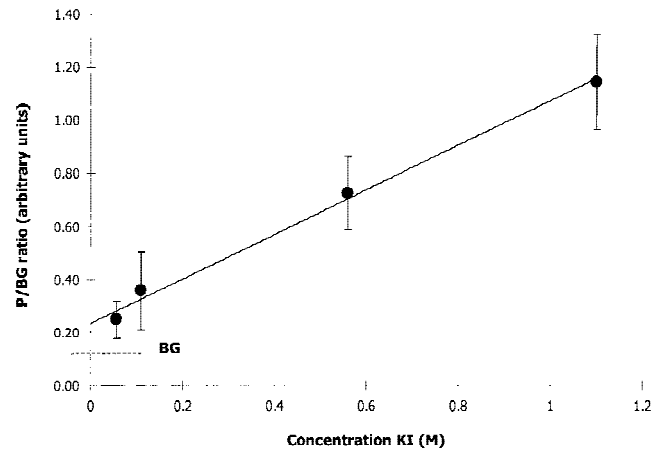


Fig. 2. Calculated regression line of KI agar gel standards. Each data point is the average \pm standard deviation of ten determinations on three gel samples. BG is the level of level of background noise.

Skin samples were chosen randomly. The site of examination on cryosections was selected such that both stratum corneum and viable epidermis could be examined in one image. Measurements started at the outermost corneocyte layer toward the viable epidermis (Fig. 1b). Similar to the KI-agar gels, the irradiated area of the skin cryosection became electron lucent as a result of XRMA, whereas the iodide X-ray count yield remained unaffected. Because only the innermost corneocyte layers could be studied, most XRMA was performed on SC and viable epidermis within a region of 4 μm from the stratum corneum–stratum granulosum interface. For this reason in neither the SC nor the viable epidermis a gradient in P/BG ratio as a function of distance from stratum corneum–stratum granulosum interface could be determined. Therefore, the data were grouped as data obtained from the SC and data obtained from the viable epidermis, and as such statistically analyzed.

XRMA data (Fig. 3) show that after both sides of the skin were exposed to HEPES buffer, P/BG ratios in neither

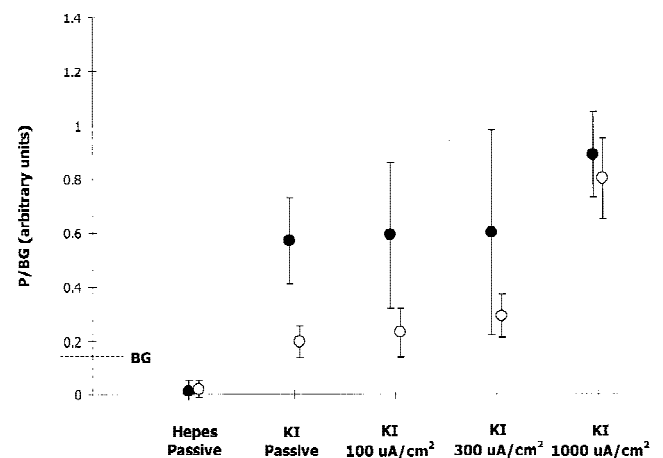


Fig. 3. Iodide peak to background ratios (P/BG) in SC (●) and viable epidermis (○) found after passive diffusion of HEPES (control), passive diffusion of KI, and KI iontophoresis using 100, 300, and 1000 $\mu\text{A}/\text{cm}^2$. Each data point is the average \pm standard deviation of 10 determinations on three different pieces of skin. BG is level of background noise.

the SC nor the viable epidermis were significantly higher than the background noise, defined in a similar way as with KI agar gels (17). When the diffusion experiment was performed with a 1.1 M KI solution on the SC side, the average P/BG ratio in the SC was found to be much higher than that in the viable epidermis (0.7 vs. 0.2 arbitrary units, respectively). Iontophoresis of KI applying current densities up to 300 $\mu\text{A}/\text{cm}^2$ did not significantly increase P/BG ratios relative to passive diffusion. However, when 1000 $\mu\text{A}/\text{cm}^2$ was applied, P/BG ratios increased significantly. Moreover, at this current density the P/BG ratios in the viable epidermis increased such that they were no longer significantly different from the P/BG ratios in the SC (both approximately 0.9 arbitrary units).

Partition Coefficient

The partition studies yielded an average organic phase/water partition coefficient (defined as C_o/C_w , where C_o and C_w are the equilibrium iodide concentrations in the organic and the aqueous phase, respectively) of 0.006 ± 0.001 .

DISCUSSION

Cryopreservation of the Epidermal Ultrastructure

In previous studies TEM used to investigate percutaneous ion transport by passive diffusion and iontophoresis mainly involved chemical preservation and precipitation (5–9). In the present study, however, skin was preserved by rapid freezing and cryohandling of the frozen sample. The local ion concentrations were determined by XRMA on tissue sections in the frozen hydrated state.

According to the results (Fig. 1a), cryopreservation revealed sufficient contrast to distinguish the SC and the viable epidermis. In the SC, layers of corneocytes were well preserved, yet neither corneosomes nor lipid lamellae could be identified. However, the observation that corneocytes were attached to each other by electron dense material may indicate that the latter structures were still present (18,19). Layers of apical corneocytes were generally detached from the rest of the SC. This may be attributed to ripping the SC when removing the cryosection from the knife after being sectioned (13). Also the viable epidermis revealed sufficient contrast to identify cells and nuclei. However, the quality of the preservation varied. Most likely, freeze artifacts are the basis for the variable fixation quality. Such artifacts are often observed beyond the maximal vitrification depth of 10–20 μm in highly hydrated tissue (20). The finding that the structure of both the SC and the viable epidermis was reasonably preserved supports our assumption that the cryopreserved skin can be used for direct examination by TEM and XRMA. This implies that staining and freeze-drying is not necessary for a proper orientation. As cryopreservation prevents the formation of artifacts from freeze-drying (21) and from the use of chemicals (10), ions can be detected at the ultrastructural level under conditions very close to those during passive diffusion and iontophoresis.

Gels with known element concentrations have been used widely as standards for quantitative XRMA on biological samples (22,23). In the present study KI agar-gel standards were used to estimate the amount of iodide in human skin, which had been subjected to passive diffusion and iontophoresis of KI. Irradiation of biological material with an electron

beam, as with XRMA, has been reported to cause damage and finally the loss of chemical elements (24). However, by measuring the P/BG ratios of one spot several successive times, it was demonstrated that the circumstances selected in the present study did not influence the iodide concentration to a measurable level.

The detection limit was defined as three times the standard deviation of P/BG ratios obtained from agar-gel to which no additional KI was added (17). Using this assumption as a condition, the lowest detectable concentration of iodide was calculated to be between 0.0 and 0.056 M. The results obtained with the KI-agar gel standards (Fig. 2) revealed a positive linear relationship between P/BG ratios and the concentration KI. This leads us to conclude that from 0.056 up to 1.1 M KI, the emission of iodide X-rays is linearly proportional to the amount of iodide in the region of exposure. This is in agreement with other authors reporting the use of gel standards (22,23).

Spatial Resolution

We used XRMA to investigate which structures in the skin are associated with percutaneous iodide transport during passive diffusion and iontophoresis. The spatial resolution in XRMA is determined by the diameter of the focused electron beam (Fig. 1b). In the present study the smallest spot size achievable, producing sufficient iodide X-ray yield and causing minimal damage to cryosections, was 140 nm. When studying iodide localization across the human skin, the SC lipid lamellae are of particular interest because these are recognized as the major barrier to percutaneous transport of hydrophilic compounds and water (1,2). The intercellular space between corneocytes is typically 40–100 nm in width (25). Thus, taking into account that the spot size used was 140 nm, it was not possible to obtain X-ray data that originated exclusively from the lipid lamellae. Therefore, data from the SC should be interpreted as partly from corneocytes and lipid lamellae, although in exposed areas of only the corneocytes iodide could be detected.

In a previous study, the iodide localization in the SC during passive diffusion and iontophoresis was investigated with fluorescence quenching (15). This study provided highly sensitive information on the presence of diffusing iodide ions in close proximity with fluorophores within SC lipid lamellae. But obtaining information on the presence of iodide in relation to other structures of the skin was not possible with this method. Hence, the results of the present study can be seen as complementary to those of that previous study.

XRMA of Human Skin

To assess whether untreated skin contained detectable amounts of iodide, we exposed skin to HEPES buffer. The results (Fig. 3) showed that no significant P/BG ratios could be found, demonstrating that skin not exposed to KI did not contain detectable amounts of iodide. Exposure to passive KI diffusion for 10 h resulted in detectable P/BG ratios. The SC contained much higher P/BG ratios than the viable epidermis. Taking the results of KI agar-gel standards into account (Fig. 2), we came to an estimated concentration of iodide in the SC of about 0.5 M, whereas the iodide concentration in the viable epidermis was not zero.

These results are in agreement with studies on the passive diffusion of potassium chromate or nickel sulfate for 18 h (4) and of mercuric chloride for 10 h (7,8). Boddé *et al.* (7,8) found mercury to be present in corneocytes and intercellular spaces of the upper SC. In the rest of the SC, mercury was primarily present in the intercellular spaces only. In the viable epidermis only traces of mercury could be found. It was suggested that the diffusion of mercury across the SC is hindered by SC lipid lamellae and corneocyte envelopes, so that ion transport would occur between these structures. It is likely that due to its strong hydrophilic character (see results octanol/water partition coefficient), iodide is present in the aqueous regions of SC intercellular spaces, hindered in diffusion through the SC by the SC lipid lamellae similarly to mercury. This suggestion is consistent with fluorescence quenching data revealing that passive iodide diffusion was associated, at least in part, with SC lipid lamellae present in the intercellular spaces (15).

The concentration of iodide found in the SC cannot be explained by this ion being localized exclusively in the intercellular spaces because the intercellular spaces comprise only 5% to 30% of total SC volume (26). Furthermore, the octanol/water partition coefficient suggests that iodide has a strong preference for aqueous phases and/or hydrophilic domains.

Corneocytes have been found to absorb large amounts of water following hydration (27,28). This finding suggests that small hydrophilic compounds may cross the corneocyte envelope and be absorbed in the corneocytes (27). The partition coefficient, the small size of the diffusing species, and the high concentration of iodide in the SC suggest that iodide might also be taken up by corneocytes. Iodide is not known to denature proteins or lipids, which make up the corneocyte envelope (29). However, it has been suggested that iodide might be associated with proteins (30). As the SC is predominantly made up of proteins such as keratin (80% by dry weight), the uptake of iodide by the corneocytes might also promote loose binding of this ion to keratin. The uptake of iodide in the corneocytes results in a much higher concentration of iodide in the stratum corneum as expected based on the partition coefficient, because iodide is not only localized in lipophilic regions but also in water-rich regions in the stratum corneum. Compared with the SC, the stratum granulosum consists of fewer proteins (about 50% by dry weight) (personal communication, P. M. Elias; unreferenced). Therefore, the difference in protein content between the stratum granulosum and the SC together with the suggested hindered iodide diffusion through the SC, due to the presence of the crystalline lipids, might explain why in the present study the SC contained a much higher concentration iodide than the viable epidermis following passive diffusion by KI. The skin had been exposed for 10 h to a 1.1 M KI solution. It means a long-term exposure to a relatively high concentration of salt. Knowing that iodide is associated with keratin, the 0.5 M exposure is not surprising.

With iontophoresis, the electrical potential gradient across the skin serves as the driving force for ion migration. Increasing electric current at constant resistance will therefore increase the flux of ions across the skin. Due to the combination of an Ag/AgI electrode with a KI solution on the cathodal side, iodide is the primary anionic current carrier in the present study. Hence, an increase of the current density is expected to increase iodide flux. The results (Fig. 3) showed

that after 10 h iontophoresis up to 300 $\mu\text{A}/\text{cm}^2$, the concentration iodide in the SC and in the viable epidermis had not increased compared with the concentration iodide after passive KI diffusion. Thus, although iodide migration through the skin increased, the concentration of iodide in the skin apparently remained unchanged. The concentration of iodide is dependent not only on the iodide migration, but also on the solubility of iodide in the stratum corneum. In our previous study in which skin was exposed to KI iontophoresis up to 300 $\mu\text{A}/\text{cm}^2$ for 10 h (15) fluorescence quenching showed that iodide inside SC lipid lamellae increased proportionally with current density (15). However, in this study only the iodide present in the intercellular regions played a role in the quenching process. Boddé *et al.* (8) and Monteiro-Riviere *et al.* (9), using TEM and chemical precipitation, found that iontophoresis at comparable current densities for 2 h leads to an increase in the concentration of mercury in the skin compared with passive diffusion. Not observing such an increase in the present study may be explained by the large variation in P/BG ratios found in the SC (Fig. 3) or to a difference in localization of the ions. Iodide is taken up by corneocytes, which "dilutes" the iodide concentration and makes it more difficult to detect a change.

Iontophoresis at 1000 $\mu\text{A}/\text{cm}^2$ leads to a significant increase of the iodide concentration in both the SC and viable epidermis (Fig. 3). Apparently, the concentration iodide in the SC was under these circumstances more or less equal to that in the viable epidermis: both approximately 0.9 M according to the results of KI agar-gel standards. These results can be explained by freeze fracture electron microscopy findings (2) reporting disorganization of SC lipid lamellae and the presence of water pools inside SC extracellular spaces following iontophoresis of 1300 $\mu\text{A}/\text{cm}^2$. With the present study, it would be suggested that such an extensive perturbation would have increased the interior of SC lipid lamellae to ions and water, which might increase the solubility of iodide in the SC structure and decrease the percutaneous diffusion barrier to hydrophilic compounds. These events cause an increase in the presence of iodide in the SC and the viable epidermis significantly and turned out to be equal to each other in this study. The finding that in the present study the concentration iodide in both the SC and the viable epidermis was found to be close to 1.1 M, the initial concentration KI in the donor compartment, emphasizes furthermore the extensive perturbation of skin ultrastructures. Because 1000 $\mu\text{A}/\text{cm}^2$ is beyond the current strength usually used *in vivo*, these findings of perturbation do not affect the applicability of iontophoresis as drug delivery technique.

Various studies have suggested that during passive diffusion ions primarily permeate the skin via a paracellular pathway (5–7). During the application of an electric field, ions were suggested to permeate primarily through appendages (3), to a less extent paracellularly (3,8,9). In the present study the suggested presence of iodide inside corneocytes of the deeper region of the SC following passive diffusion and iontophoresis hints at a possible transcellular pathway for percutaneous iodide transport. Although this hypothesis may sound contradictory to what has been suggested so far, iodide is a relatively small compound and is more water soluble than compounds studied before, such as nickel (nickel sulfate) (6) and mercury (mercuric chloride) (6–9). As a consequence, iodide would be more likely to cross the corneocyte envelope.

In addition, in the present study the skin was exposed for a much longer period than in various other studies (5,6,9), allowing more ions to be taken up by corneocytes.

Still, whether hypothesized transcellular ion transport is significant compared with transport via other pathways is not known because no information could be obtained on skin structures smaller than 140 nm, no appendages were studied, and the skin had not been studied as a function of exposure time to KI. Elucidating the extent of this suggested transport is a challenge for future research.

CONCLUSIONS

In conclusion, the present study showed that cryopreservation retains the morphology of the skin sufficient to allow direct examination by TEM. Examination of cryosections under cryoconditions offers the possibility of quantifying the distribution of migrated (iodide) ions inside the skin by XRMA, under conditions very close to those extant during diffusion and iontophoresis. Limitations in spatial resolution, however, made it impossible to obtain information on structures smaller than 140 nm. We could show that after passive diffusion, iodide was mainly present in the SC whereas little iodide could be demonstrated in the viable epidermis. Iontophoresis up to 300 $\mu\text{A}/\text{cm}^2$ did not significantly affect this distribution. Iontophoresis at 1000 $\mu\text{A}/\text{cm}^2$, however, was found to perturb skin structures such that the amount of iodide increased dramatically and made it possible for iodide to be equally distributed over the SC and viable epidermis. Finally, the present study suggests the possibility of transcellular percutaneous iodide transport. Learning to what extent possible transport via this pathway would contribute to the total percutaneous ion transport will be a challenge for future research.

ACKNOWLEDGMENTS

The authors would like to thank Dr. Russell O. Potts, Cygnus Inc. (Redwood City, CA) for his critical evaluation and Dr. Peter M. Elias, VA Medical Center (San Francisco, CA) for providing insightful information. This study is part of a PhD program at the Leiden Amsterdam Center for Drug Research and was sponsored by Cygnus Inc. (Redwood City, CA).

REFERENCES

1. R. O. Potts and M. L. Francoeur. The influence of stratum corneum morphology on water permeability. *J. Invest. Dermatol.* **96**:495–499 (1991).
2. W. H. Craane-van Hinsberg. *Transdermal Peptide Iontophoresis*, Ph.D. dissertation, Leiden University, The Netherlands, 1994.
3. N. G. Turner and R. H. Guy. Iontophoretic transport pathways: Dependence on penetrate physicochemical properties. *J. Pharm. Sci.* **86**:1385–1389 (1997).
4. B. Forslind, T. G. Grundin, M. Lindberg, G. M. Roomans, and Y. Werner. Recent advances in X-ray microanalysis in dermatology. *Scan. Microsc.* **2**:687–695 (1985).
5. C. A. Squier and C. A. Lesch. Penetration pathways of different compounds through epidermis and oral epithelia. *J. Oral. Pathol.* **17**:512–516 (1988).
6. H. Sharata and R. R. Burnette. Effect of dipolar aprotic permeability enhancers on the basal stratum corneum. *J. Pharm. Sci.* **77**:27–32 (1988).
7. H.E. Boddé, M. A. M. Kruithof, J. Brussee, and H. K. Koerten. Visualization of normal and enhanced HgCl_2 transport through human skin *in vitro*. *Int. J. Pharm.* **53**:13–24 (1989).
8. H.E. Boddé, F. H. N. de Haan, L. Kornet, W. H. M. Craane-van Hinsberg, and M. A. Salomons. Transdermal iontophoresis of mercuric chloride *in vitro*; electron microscopic visualization of pathways. *Proceed Intern. Symp. Control. Rel. Bioact. Mater.* **18**: 301–302 (1991).
9. N. A. Monteiro-Riviere, A. O. Inman, and J. E. Riviere. Identification of the pathway of transdermal iontophoretic drug delivery: Light and ultrastructural studies using mercuric chloride in pigs. *Pharm. Res.* **11**:251–256 (1994).
10. A. J. Morgan. Preparation of specimens: Changes in chemical integrity. In M. A. Hayat (ed.), *X-Ray Microanalysis in Biology*, McMillan, London, 1980 pp. 65–166.
11. C. Cullander. What are pathways of iontophoretic current flow through mammalian skin? *Adv. Drug Del. Rev.* **9**:119–135 (1992).
12. R. J. Condron and A. T. Marshall. A comparison of three low temperature techniques of specimen preparation for X-ray microanalysis. *Scan. Microsc.* **4**:439–447 (1990).
13. R. R. Warner, C. M. Mark, and D. A. Taylor. Electron probe analysis of human skin: Determination of the water concentration profile. *J. Invest. Dermatol.* **90**:218–224 (1988).
14. R. R. Warner, R. D. Bush, and N. A. Ruebusch. Corneocytes undergo systematic changes in element concentrations across the human inner stratum corneum. *J. Invest. Dermatol.* **104**:530–536 (1995).
15. L. A. R. M. Pechtold, W. Abraham, and R. O. Potts. The influence of an electric field on ion and water accessibility to stratum corneum lipid lamellae. *Pharm. Res.* **13**:1168–1173 (1996).
16. J. J. McCarthy and F. H. Schamber. Least squares fit with digital filter; a status report. In K. F. J. Heinrich, D. E. Newbury, R. L. Myklebush, C. E. Fiori (eds.), *Energy Dispersive X-Ray Spectroscopy*, National Bureau of Standards, Washington DC, 1977 pp. 273–297.
17. R. L. Pecksook, L. D. Shields, T. Cairns, and I. G. McWilliam. *Modern Methods of Chemical Analysis*, 2nd ed., John Wiley & Sons, New York, 1976 p. 264.
18. M. M. G. Wijdeveld, H. K. Koerten, J. J. M. Onderwater, D. T. Parrott, and J. A. Bouwstra. Visualization and electron diffraction on cryo-sections of stratum corneum: A utopia? *J. Microsc.* **183**:223–230 (1996).
19. G. S. K. Pilgram, A. M. Engelsma-van Pelt, J. A. Bouwstra, and H. K. Koerten. Electron diffraction provides new information on human stratum corneum lipid organization studied in relation to depth and temperature. *J. Invest. Dermatol.* **113**:403–409 (1999).
20. H. Y. Elder, C. C. Gray, A. G. Jardine, J. N. Chapman, and W. H. Biddlecombe. Optimum conditions for cryoquenching of small tissue blocks in liquid coolants. *J. Microsc.* **126**:245–266 (1986).
21. H. K. Hagler and L. M. Buja. Effect of specimen preparation and section transfer techniques on the preservation of ultrastructure, lipids and elements in cryo-sections. *J. Microsc.* **141**:141–152 (1986).
22. A. T. Sumner. Gelatin standards for elemental quantification in biological X-ray microanalysis. *Scan. Microsc.* **4**:429–438 (1990).
23. A. Warley, J. Stephen, A. Hockaday, and T. C. Appleton. X-ray microanalysis of HeLa S3 cells. I instrumental calibration and analysis of randomly growing cultures. *J. Cell Sci.* **60**:217–229 (1983).
24. J. A. Chandler. X-ray microanalysis in the electron microscope. In A. M. Glauert (eds.), *Practical Methods in Electron Microscopy*, Elsevier/North-Holland Biomedical Press, Amsterdam, 1977 pp. 327–376.
25. G. Plewig and Th. Jansen. Size and shape of corneocytes: Variation with anatomic site and age. In K. P. Wilhelm (ed.), *Bioengineering and the Skin: Skin Surface Imaging and Analysis*, CRS Press, Boca Raton, 1996.
26. P. W. Wertz and D. T. Dowling. Glycolipids in mammalian epidermis: Structure and function in the water barrier. *Science* **217**: 1261–1262 (1982).
27. D. A. van Hal, E. Jeremiasse, H. E. Junginger, F. Spies, and J. A. Bouwstra. Structure of fully hydrated human stratum corneum: A freeze-fracture electron microscopy study. *J. Invest. Dermatol.* **106**:89–95 (1996).
28. M. S. Roberts and M. Walker. Water: The most natural penetration enhancer. In K. A. Walters and J. Hadgraft (eds.), *Pharmaceutical Skin Penetration Enhancement*, Marcel Dekker, New York, 1993 pp. 1–30.
29. L. S. Goodman and A. Gilman. *The Pharmacological Basis of Therapeutics*, Macmillan, New York, 1958.
30. J. Steinhardt and J. A. Reynolds. *Multiple Equilibria in Proteins*, Academic Press, New York, 1969.